Internal Blast Measurements in a Model of the Pantex Damaged Weapons Facility

By

J. C. Hokanson, E. D. Esparza, W. E. Baker and N. R. Sandoval,
Southwest Research Institute

ABSTRACT

The Damaged Weapons Facility (DWF), planned for construction at the Pantex Plant, will consist of several rooms and interconnecting corridors. It is being designed to essentially completely contain explosive effects in the event of an accidental explosion during weapon disassembly. Because of the complex geometry of the facility, the rational prediction of initial and later reflected shock wave loading, and the longer-term gas pressure loading, is very difficult. Accordingly, a one-eighth scale, overstrength, steel "loads" model of the facility has been built and tested. Tests include detonations within the model of various weights and types of spherical and cylindrical explosives, at several charge locations within the high bay area of the facility. This paper summarizes shock and gas pressure measurements taken within the model, and compares test results to current methods for estimating these transient pressures and to data from other investigators.

INTRODUCTION

General

This paper summarizes results of a two-phase test program conducted by the staff of Southwest Research Institute under Purchase Order No. F0913400, for Mason and Hanger-Silas Mason Company, Inc., Pantex Plant, Amarillo, Texas.

The work involved the design, preparation of construction drawings, fabrication, instrumentation, and internal blast testing of a one-eighth geometric scale model of the Damaged Weapons Facility (DWF) planned for construction at the Pantex Plant. The full-scale facility, which is to be used as a disassembly facility for damaged weapons, is being designed for Department of Energy, Amarillo Area Office, by the firms of Gibbs and Hill, and Ammann and Whitney. Since these weapons contain high explosives as well as toxic material, their disassembly must be performed within a structure which in the event of the occurrence of an accidental detonation, will contain, within acceptable limits, the explosive and toxic materials output.

The Damaged Weapons Facility will consist of several rooms and interconnecting corridors. The disassembly of a weapon will take place in the main room or bay. This room is fully enclosed except for an access opening to surrounding staging areas, corridors, and equipment and personnel blast locks. Methods for determining the blast loads produced by spherical charges which are detonated within fully enclosed cubicle type bays are well known (Refs. 1 and 2). However, only a minimal amount of data are available pertaining to the evaluation of the blast loads and overpressures which leak out of a bay into the adjoining confined areas.

To determine these latter blast loads, a series of tests has been conducted. These tests included the initiation of various explosive charges within a one-eighth scale model of the Damaged Weapons Facility and recording the magnitude of the resulting blast overpressures, impulse and thermal variations. The data obtained from these tests will enable the verification (or nonverification) of the estimated blast loads used for the building design (Phase I). Also, the test results provide an insight into internal blast loads produced by (1) multiple charges, (2) charge geometry, (3) charge confinement and (4) TNT equivalency (Phase II).

Purpose and Objectives

The primary purposes of the tests in Phase I were to obtain measurements of the blast and gas pressure loads, both within the high bay where explosions may occur, and within corridors and staging bays adjacent to the high bay. All but one of the explosive charges detonated in this phase were single PBX 9404 spheres weighing about 0.990 lb (this represents 507 lb in full scale). The charge location was varied, as well as the pressure measuring stations. Tests were replicated three times to determine reproducibility of measured dynamic loads.

The objectives for Phase II were the determination of internal blast loads associated with:

1. "TNT equivalency" of PBX 9404, PBX 9502, and Pentolite;
2. Multiple charges;
3. Short cylindrical charges;
4. Lightly cased charges.

In support of the first of these objectives, there was also a requirement for measuring heats of combustion for explosives to be tested in this program, as well as explosives for which there was an extensive data base of internal explosion measurements.

An additional objective during this phase was to obtain better transient thermal measurements by use of fast-response calorimeters, and to use these measurements to predict temperature-time histories for critical components in the prototype structure.

Paper Content

In following sections, we describe the design and construction of the model, give our plan for instrumentation, describe the plan for reduction of the many channels of data recorded during each test, and give the test plan for both phases of the tests. Then, test results are summarized. The paper concludes with a discussion of the test results. A reference list is appended. Much more complete descriptions of this internal blast project appear in Ref. 3 and 4 for Phase I and Ref. 5-7 for Phase II.

SCALING

The Hopkinson-Cranz scaling law for air blast waves from explosive sources (Ref. 8) predicts that the entire history of shock loading of a complex structure should scale properly in subscale experiments, provided that:

1. Exact geometric similarity is maintained,

2. All times scale in exactly the same proportion as the geometric (length) scale factor λ,

3. Types of explosive sources are identical and total source energy E scales as λ^3, and

4. Initial atmospheric ambient conditions are unchanged.

Furthermore, References 9 and 10 show that explosions within vented or unvented containment structures will generate long-term (quasi-static) pressures whose amplitudes and durations (when vented) also scale according to the Hopkinson-Cranz law.

The implications of the blast scaling law are as follows:

1. At similar locations and similar scaled times, pressure amplitude and velocities are identical in model and full-scale tests.

2. Because times are compressed by the scale factor λ, shock arrival times, pressure rise times, overpressure durations, and all characteristic times in complex pressure-time histories scale by λ.

3. Specific impulses also scale as λ, because the amplitudes (pressures) are unchanged and the durations scale as λ.

Inherent in the Hopkinson-Cranz law is the assumption (and proof by many, many tests) that, for the very rapid shock loading and still rapid gas pressure rise processes in contained high explosive loading, heat transfer processes lag so greatly that they have insignificant effect on the transient loads.* The scaling of the complex process of heat transfer by radiation, convection and conduction is very difficult (see Chapter 12 of Ref. 8), and obeys quite different scaling laws than for the pressure loads from contained explosions.

Basically, the model of the DWF which we built and are testing maintains close to the exact geometric internal shape of the full-scale DWF design. However, outer wall, roof and floor thicknesses are not exactly geometrically scaled, but are instead designed for strength to withstand many scaled internal explosions with no damage. No attempt whatever was made to scale or model heat transfer processes in model design and construction.

*Eventually, even the quasi-static pressure within a gas-tight container will very nearly equilibrate, as the hot explosion gases and compressed air mix and cool by heat transfer through the container walls.

Basically, the model of the DWF which we built and are testing maintains close to the exact geometric internal shape of the full-scale DWF design. However, outer wall, roof and floor thicknesses are not exactly geometrically scaled, but are instead designed for strength to withstand many scaled internal explosions with no damage. No attempt whatever was made to scale or model heat transfer processes in model design and construction.

There is ample evidence that the Hopkinson-Cranz blast scaling law applies for very small geometric scale factors λ (see Ref. 8). So, the choice of λ is dictated by other factors. As the scale factor becomes smaller, the required frequency response for blast transducers and recording systems must be increased proportionally, because all times are also shortened by λ. Also, as model size decreases, access to the model becomes more difficult. These negative factors must be weighed against reduced construction cost with smaller size. The choice of $\lambda = 1/8$ for this model was dictated primarily by the need for internal access to change model configuration and to inspect, replace or rearrange instrumentation between tests. Someone had to be able to crawl inside the model, and that would have been impossible at a smaller scale.

MODEL DESIGN AND CONSTRUCTION

Model Design

All-welded construction was chosen for this model, because of strength, economy in construction and ease of making the model pressure-tight. The basic construction material was chosen to be a pressure vessel steel, ASTM A 537 Class 1. This material has high yield strength and ductility, even at low temperatures. It also can be welded in thick sections with little loss in material strength and ductility.

We conducted some limited analyses to predict blast loads and response of elements in the structures, to allow us to size the steel plate thicknesses for various parts of the structure.

Most of the blast loading predictions were made for the surfaces of the high bay area, using worst-case (nearest charge locations) for each surface. The methods for predicting local and average peak overpressure and specific impulse loading are described in detail in Reference 2. Details appear in Ref. 1. Quasi-static pressures were also predicted from a curve in Reference 2, using the maximum charge weight and the volumes of the high bay area for one pressure, and the entire internal volume of the model for another pressure.

Using the maximum calculated blast and quasi-static loads within the high bay area, plate thicknesses were sized assuming elastic beam strip theory, clamped-clamped boundary conditions, and a factor of safety (FS) of 1.5, based on static yield strength for the A 537 Class 1 steel. Scaled pressure-impulse (P-i) diagrams from Reference 11 were used for these calculations. The results showed that h = 3 inches was adequate for all surfaces in this part of the structure. Details appear in Ref. 1.

Calculations of blast loads within other parts of the structure are very questionable (which is, indeed, the reason for this program). So, to achieve a conservative design and to allow choice of a suitable hydrotest pressure,

we established Dynamic Load Factors for the heavily-loaded high bay structural elements, based on the vibration frequencies of appropriate beam strips, and then computed equivalent static pressures to give the same maximum stresses, using again the safety factor of 1.5. The recommended hydrotest pressure was P_T = 210 psi. Based on this pressure, plate sizes were chosen for the remainder of the model. These were 1.5 inches for walls outside of the high bay, and 2.0 inches for roof outside the high bay. Although there are no good methods for predicting blast loads outside the high bay area, we felt that we could obtain at least order of magnitude estimates by exercising a two-dimensional blast wave code and representing the three-dimensional model structure by a two-dimensional analog. The results of these calculations could give a rough idea of blast pressures and rise times, and thus help in selection of appropriate transducers, as well as indicate possible areas of blast focusing causing local high pressures. The results of these calculations appear in Appendix C of Ref. 1. Although the absolute numbers were not expected to correlate well with test data, relative amplitudes between the high bay area and other areas were helpful in planning our instrumentation. They were also comforting to the designers, because no high local overpressures were predicted outside the high bay area.

The final design of the model evolved on the basis of the above design calculations; the need for access to all outer surfaces of the model for installing and for changing instrumentation; and the practical requirements for welding, assembling, inspection, and stress relief. A support structure allowing access from below was designed as a welded grillage of deep section I-beams, with seven large access holes cut through the webs. In the model itself, the design allowed subassembly of units, which were then welded together for final assembly. The method and sequence of construction was planned to minimize welding distortions, and to allow complete nondestructive inspection of critical welds.

In the final design, there are two hinged manhole covers for access, many transducer holes, sliding doors for the equipment and personnel locks which can be bolted in place in the closed position or held open, and a small vent pipe which is normally closed, but can be opened through a pneumatically actuated valve.

Model Construction

The model was fabricated at Southwest Research Institute. Steel plate was cut to size, beveled as needed, and welded into subassemblies using machine and hand welding equipment and methods. All "outer envelope" welds which must withstand significant blast and quasi-static pressure loads were fully inspected using approved methods of nondestructive inspection. Any critical flaws were ground out and rewelded.

The model was assembled in several subassemblies, which were separately stress relieved. These two major subassemblies were then welded together, and other small parts welded in place. While still in the welding shop, the model was hydrostatically tested to 210 psig. It was then painted and installed at our test range. The completed model is shown in Fig. 1 and 2.

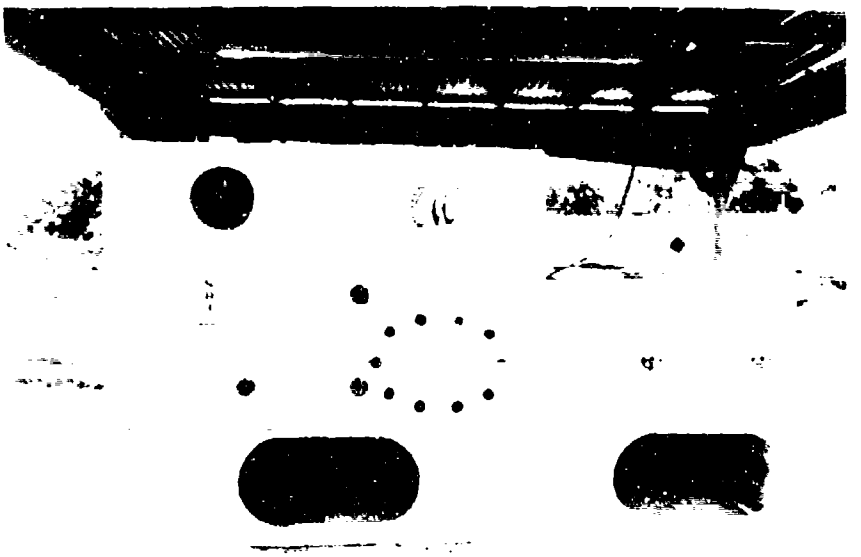

Figure 1. Completed Model Installed at Test Range

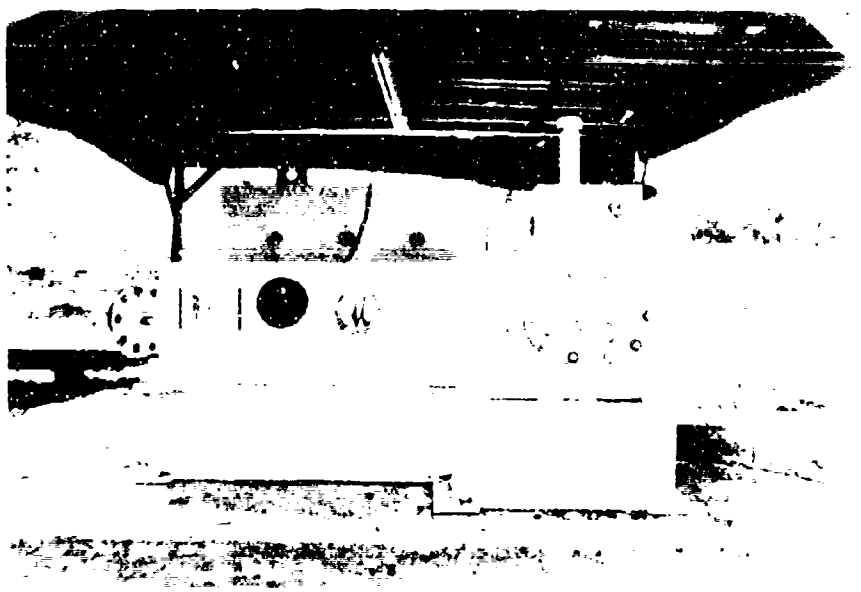

Figure 2. Completed Model Installed at Test Range

INSTRUMENTATION

In these tests, three types of transient measurements were made during Phase I:

1. Blast pressure
2. Gas pressure
3. Temperature.

In addition, heat fluxes were measured during Phase II. There were 53 measurement locations during Phase I, increased to 63 during Phase II. These locations are shown schematically in Fig. 3 and 4. On any one test, only certain locations were instrumented. The rest of the sensing locations were sealed with blind covers to maintain model pressure tightness.

Blast Pressure

The majority of the measurements made were blast pressures. The transducers selected for these measurements are made by PCB Piezotronics, Inc., and are miniature dynamic sensors specifically designed for blast wave measurements which require very high frequency response. Two basic models were used, Model 102 and Model 109A. All Model 102 transducers have the same mechanical configuration but have four different ranges (250; 1,000; 5,000; and 10,000 psi). For those gage locations very close to the charge, Model 109A (80,000 psi) transducers were used because of the higher blast pressures expected. This higher range transducer does differ in mechanical configuration from the lower range transducers.

Each PCB transducer utilizes an acceleration compensated, quartz, piezoelectric, pressure sensing element coupled to a miniature source follower within the body of the transducer. This micro-electronic amplifier converts the high impedance output of the quartz element into a low impedance, high level output signal. Regardless of range or configuration, all of these transdcuers have a rise-time capability of one microsecond.

Recording of all blast pressure data was done on two, 14-track, Wideband II FM tape recorders at a speed of 60 ips. The data bandwidth (-3db) at this recording speed is 0-250 kHz.

Gas Pressure

For gas pressure measurements made at locations where the blast pressure amplitude was expected to be only slightly higher than the quasistatic gas pressure, Endevco Model 8510M transducers, with a range of 500 psi, were used. At gas pressure locations where high amplitude blast pressures were expected (primarily in the high bay) Endevco Model 8511A with a range of 2,000 psi, and Kulite Model HKS-375 with a range of 5,000 psi were used to sense the higher gas pressure.

All of these transducers use a four-arm Wheatstone bridge diffused into a silicon diaphragm. These piezoresistive transducers feature greater than 100 mV full-scale output voltage, high resonant frequency, good linearity, and static pressure response. These transducers are capable of recording blast pressures.

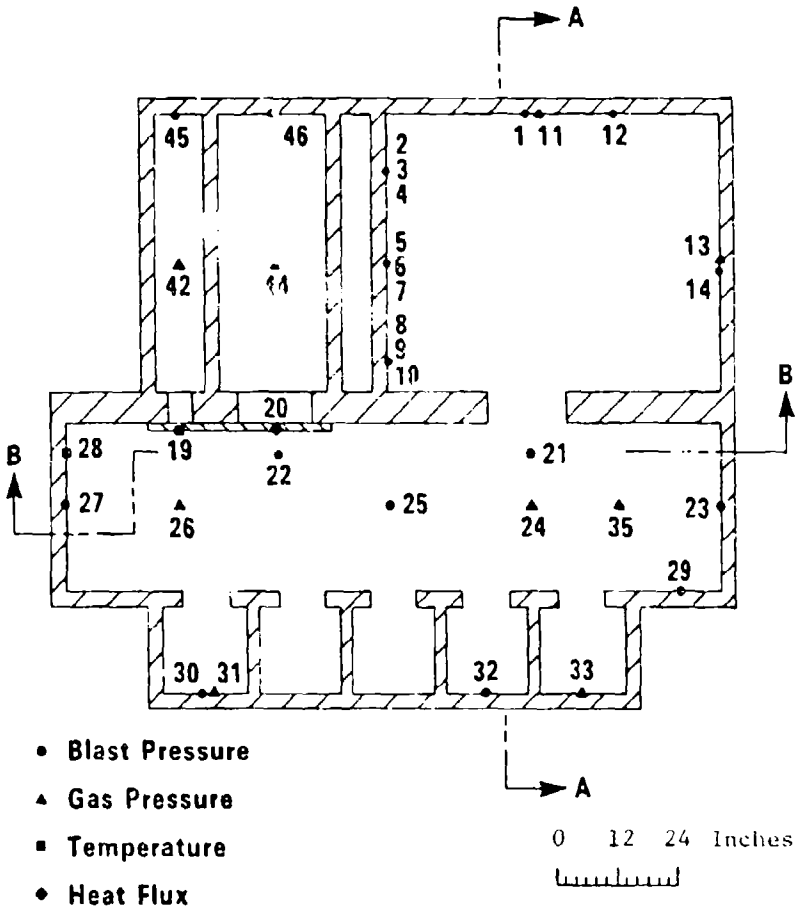

Figure 3. Transducer Locations, Plan View

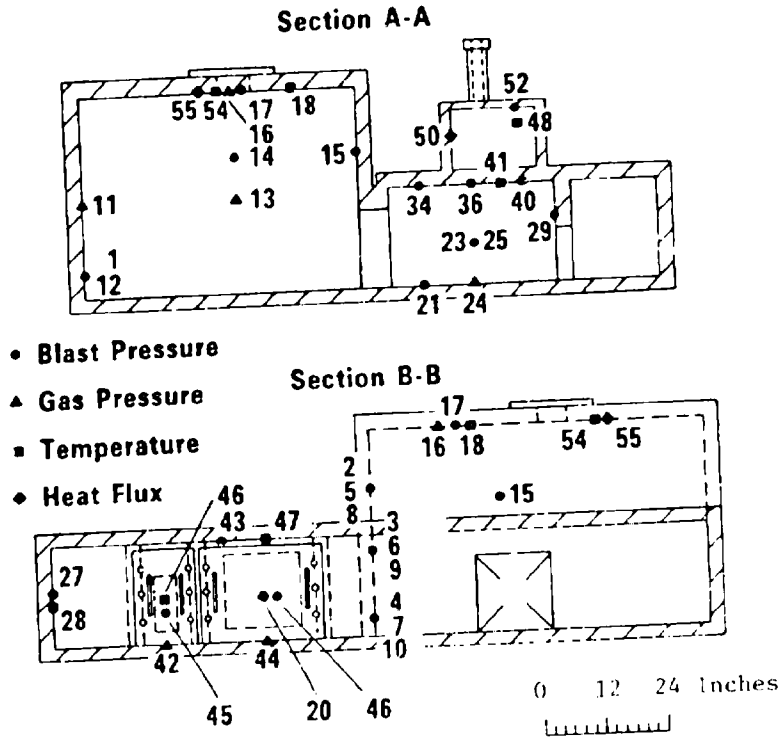

Figure 4. Transducer Locations, Vertical Sections

However, because of their static pressure response capability, they were set up to sense the gas pressure rise within the model structure, while at the same time providing a reasonable survival rate to the higher blast pressures.

Bridge power and output signal amplification was provided with Vishay Model 2310 signal conditioning amplifiers. These units accept low-level signals from strain gages, piezoresistive transducers, thermocouples, etc., and condition and amplify them into high-level outputs suitable for multi-channel magnetic tape recordings.

Recording of all gas pressure data was made on a 14-track, Intermediate band, FM tape recorder at a speed of 30 ips. The data bandwidth (±1db) at this recording speed is 0-10,000 Hz. This bandwidth was more than sufficient to record the gas pressure data.

Temperature and Thermal Flux

Although some inner surface temperature measurements were made during Phase I testing, and more temperature and thermal flux measurements during Phase II, the primary thrust of the testing was to obtain pressure measurements. So, we do not detail the instrumentation for recording transient temperatures and thermal fluxes. See Ref. 3-7 for details.

Playback Electronics

The test data recorded in both phases were played back and digitized using the system shown in Figure 5, to produce the data plots. Up to four channels of data were played back at one time through the analog filters into a Biomation Model 1015 four-channel transient recorder. This recorder digitizes the incoming analog signals at sample intervals of 0.01 milliseconds or greater. Since this unit has four separate analog-to-digital (A/D) converters, the samples for each of the four data channels are time correlated. The maximum number of samples which can be taken is 1024 per channel. The A/D units are 10 bit units, which means that the analog signals are digitized with a resolution of one part in 1024 of the full-scale voltage setting. The minimum full-scale voltage setting is 0.1 volts.

Once the test data (or calibration pulses) are properly formatted in digital form, the DEC 11/23 computer extracts the data from the transient recorder memory through the CAMAC* data buss and stores them on an eight-inch flexible diskette. A graphics terminal is used to display each data trace for verification.

The stored data on the diskettes were read into a DEC 11/70 minicomputer; then, the appropriate data processing plots were prepared using a Printronix 300 printer/plotter.

DATA REDUCTION

General

The test data were digitized using the equipment described in the previous section with the following procedure. The calibration signals, 1 kHz, 1 volt

*Computer Automated Measurement and Control ANSI/IEEE-583 Buss

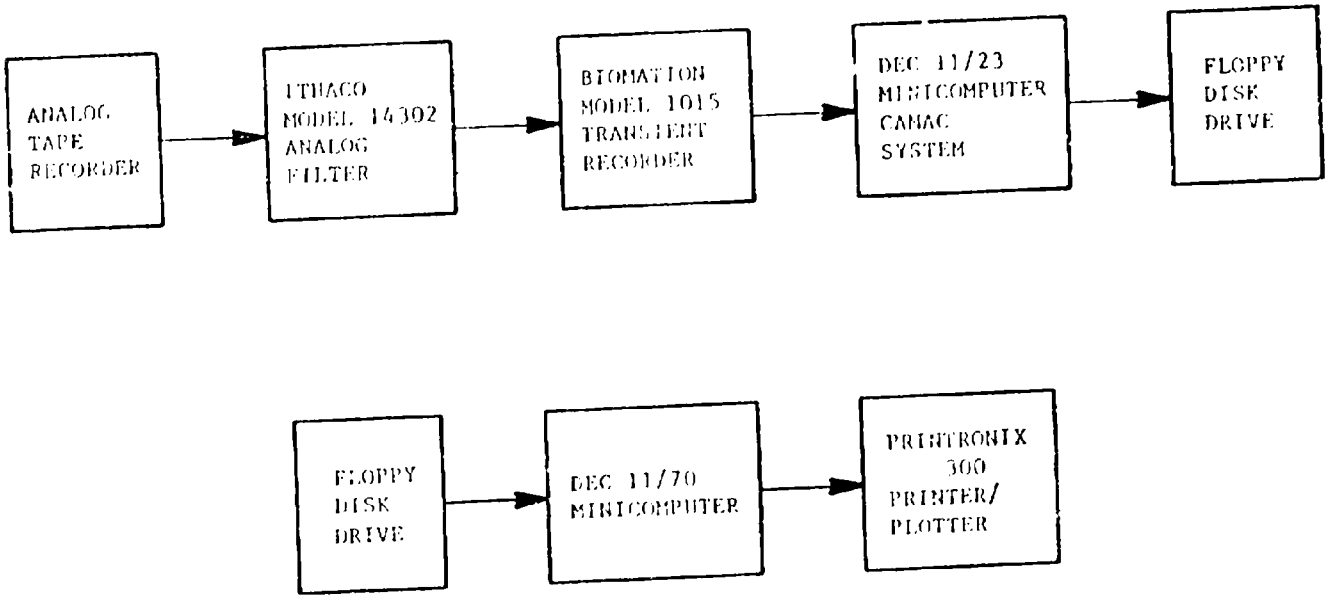

Figure 5. Test Data Playback System

p-p, recorded on each tape recorder channel prior to each test, were digitized by the Biomation unit and transferred to the 11/23 computer. The analog filters were set to a low pass cutoff frequency of 200,000 Hz for the calibration signal playback. The digitized calibration signal was analyzed to establish the factor required to convert the test data to engineering units.

The calibration factor was calculated individually for each gage on each test. Then the analog data were played into the Biomation recorder. The filters were generally set at a low pass cutoff frequency of 2000 Hz for the gas pressure gages and 2000 Hz for the blast pressure gages in the low bay. The filters were generally set at a low pass cutoff frequency of 200,000 Hz for the blast pressure gages in the high bay. To ensure that all data channels were time correlated, the signal which caused the charge to explode was recorded on channels 1 and 2 of each tape recorder. This signal, which we call time zero, was also digitized unfiltered in channel 1 of the Biomation recorder each time data were played back. The data digitized by the Biomation have units of counts. The data amplitude in engineering units of psi is then determined using calibration data for each transducer and the calibration factor also.

Extraction of Engineering Design Parameters from the Pressure Traces

The pressure records digitized as described above were examined to obtain certain parameters useful in the design of a structure loaded by an internal explosion. The parameters desired are:

- o quasi-static pressure, P_{QS}
- o shock pressure, P_S
- o shock impulse, I_S
- o duration of shock loading, D_S.

The definitions of these parameters are given in Figure 6. The maximum quasi-static pressure is quite difficult to define because it is obscured by the initial shock and the first few reflected shocks. Obviously, several reflections must take place before an irreversible process attenuates the shocks and converts the energy into the quasi-static pressure. We have decided to set the P_{QS} by examining the record and locating the time at which the shocks appear to be well attenuated. The amplitude at this time is then defined as the quasi-static pressure. This point also defines the duration of the shock loading. If we assume that the quasi-static pressure builds linearly from zero to P_{QS}, then the shock impulse is defined as the integral of the net pressure amplitude above the ramp increase. This is shown in Figure 6 as the shaded region of the curve. The shock pressures are then the amplitudes of the initial shock and the first few peaks, again above the ramp increase in the quasi-static pressure.

The quasi-static pressures are estimated using the same techniques as the blast pressure records. The shock pressure, impulse, and duration were not extracted from these records.

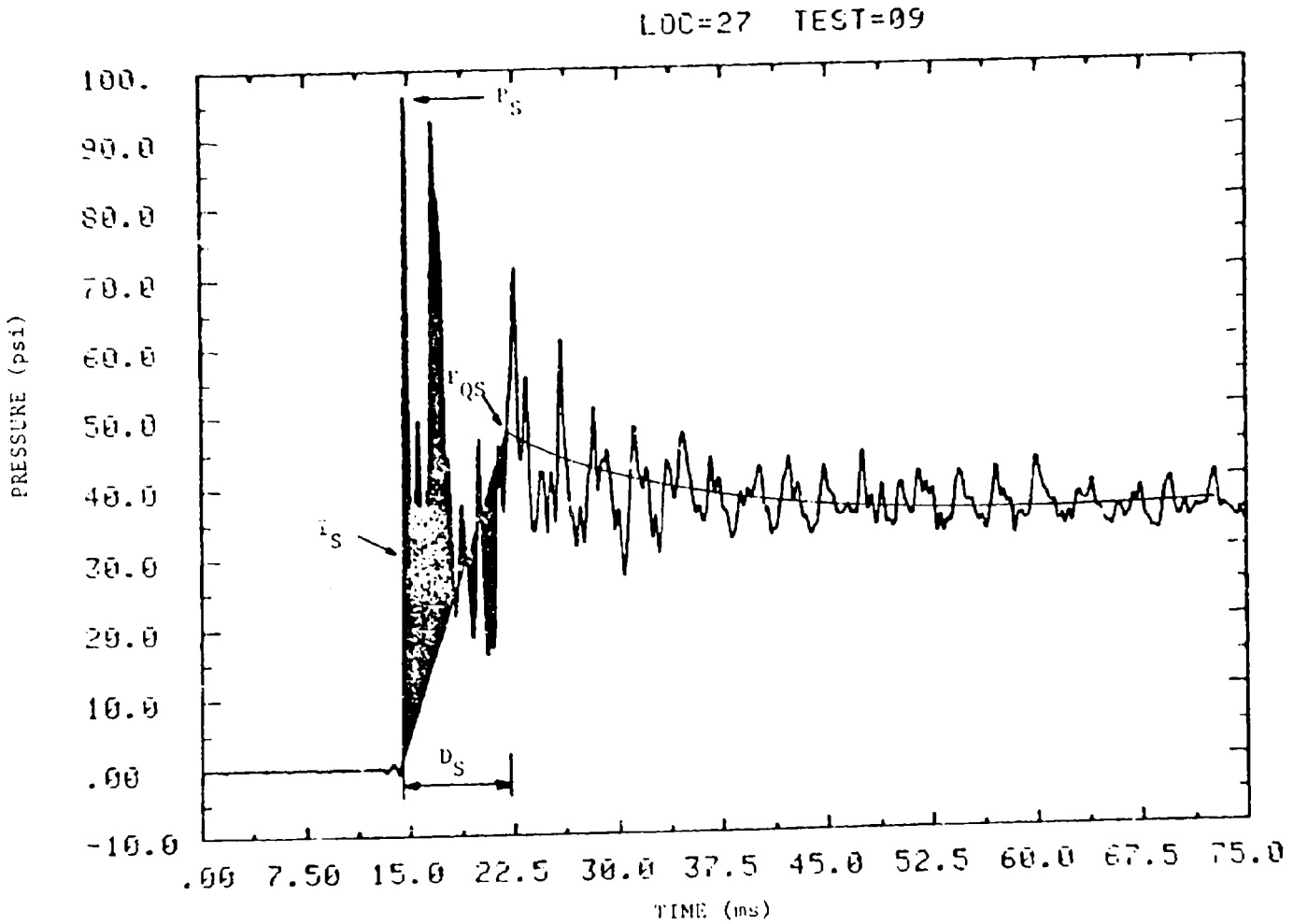

Figure 6. Definition of Parameters Extracted from the Blast Pressure Traces

TEST PLAN

Test Procedures

All of the explosive charges used in this program were provided by Mason and Hanger. Mason and Hanger also conducted a number of tests to determine a reliable method of initiation so that output (breakout) from the spherical charges was as simultaneous as possible. (See Ref. 12.) Prior to conducting the Phase I experiments, 12 PBX-9404 charges, two pentolite charges and two TNT charges were selected at random and were assembled under the direction of personnel from Pantex. The assembly consisted of gluing the Reynolds Industries RP-2 exploding bridgewire detonator into the specially machined cavity in each charge. Extra care was taken when assembling the TNT charges, since these charges had a small PBX-9404 pellet at the bottom of the cavity (to provide reliable and consistent high order ignition) which has to be properly seated. These assembly procedures were followed throughout the test program.

Each test began with the preparation of a data sheet which defined the gage location, gage serial numbers, amplifier gain, charge location, and other test information for the range personnel. The technicians would then install the gages in the model and connect them to the instrumentation system. If a gage had already been installed, then all exposed wiring was inspected and corrected if necessary. The gages were checked for continuity at the amplifier to ensure that each channel was properly connected and that the transducer was electrically sound. The test prolog and the 1.0 volt, 1 kHz calibration were then recorded on each of the three analog tape recorders.

A technician then examined each transducer from the inside of the model. Any debris on the transducer diaphragm was carefully cleaned off. The Endevco gas gages have a recessed diaphragm. The cavity on the exposed face of the transducer must be filled with an opaque grease to protect the transducer and to prevent a photoelectric response from the light emitted from the fireball. This cavity was filled with a syringe prior to each test (after Test 4) with the grease provided by Endevco. A thin coat of Dow Corning DC-4 was applied over the diaphragm for thermal shielding. The last step in preparing for the test was to suspend the charge at the location specified for the test. This was accomplished by placing the charge in a portion of a fish net, and hanging the net from one of several nuts which had been welded to the roof of the high bay. Charge locations are shown in Fig. 7. Nuts welded to strategic points on the floor provided additional tie-down points to ensure that the charge was suspended as close as reasonably possible to the desired charge location. Still photographs of the suspended charge were taken before the two manhole doors were closed. The pneumatic valve used to relieve the pressure in the model after a test was checked to ensure that the valve was closed. The range was then cleared of all personnel.

At this point, the tape recorders were placed in the record mode, and the charge was fired. The tape recorders were left on for a minimum of 10 seconds before being turned off. Once all recorders had been shut down, the pneumatic valve was opened remotely, and the pressure in the model was allowed to vent. The lead technician then checked the current weather conditions and made the appropriate entries on the data sheet. The manhole covers were opened, and fans were placed in front of the openings to clear the detonation products from the model. The fans were run for one hour before any personnel had access to the

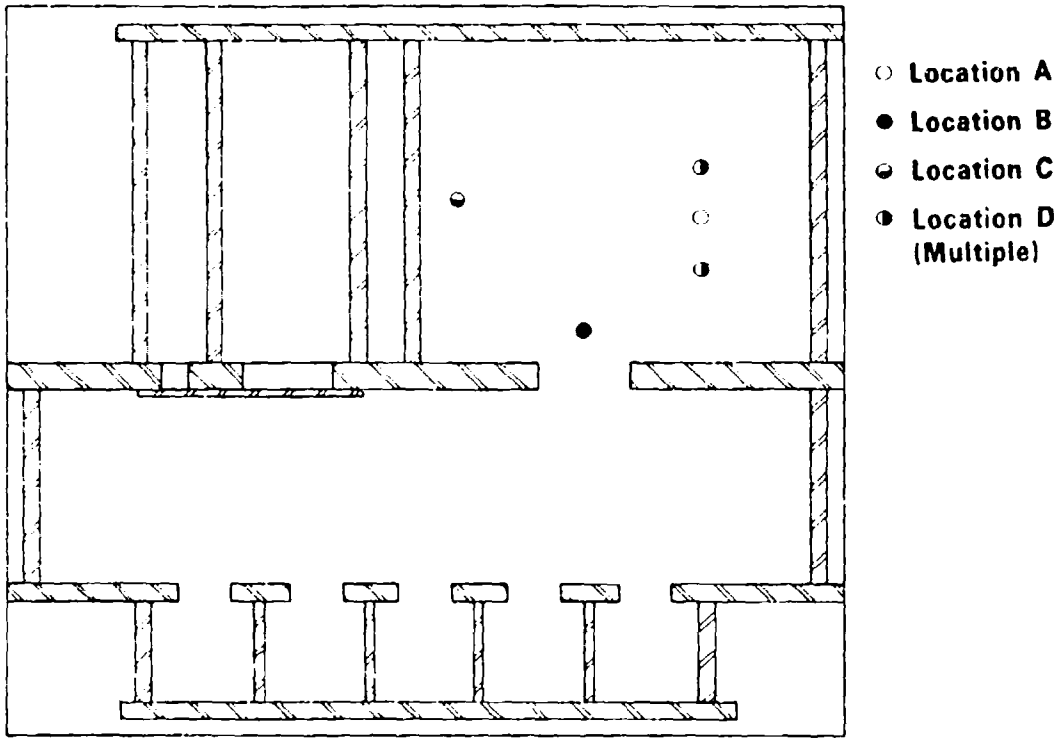

Figure 7. Charge Locations

inside of the model. Then the exterior and interior of the model were examined for any signs of damage and/or gas pressure leakage.

Phase I Test Matrix

The 12 tests planned for Phase I are summarized in Table 1. Test 0 was planned for a leakage check of the model, but also yielded some useful transient pressure data, so it is included in the matrix. As noted earlier, the primary purpose of this phase was to define transient and long-term pressure loads in areas out of the high bay, so instrumentation was concentrated there for most tests in this phase.

Phase II Test Matrix

This phase included 37 tests, arranged according to the matrix in Table 2. Here, the high bay area was instrumented more completely. Note that, in both phases, tests in any specific configuration were replicated at least once, and usually twice, to determine repeatability of measurements. For Tests 40-45, the model was modified by welding a closure over the high bay door, to lower the internal volume and increase quasi-static pressure.

TEST RESULTS AND DISCUSSION

We recorded useable data on most recording channels on all tests, except during Tests 12, 13 and 22 when a tape recorder malfunctioned, or during most of the tests when transducers were damaged by severe thermal, shock, or fragment impact loads.

The reduced data, in a format of one time history per page, are truly voluminous, and appear in Ref. 4, 6, and 7. They are much too extensive to reproduce here. Typical blast pressure records are shown in Fig. 8, and gas pressure records in Fig. 9. The multiple shocks were quite pronounced in the high bay area, but were markedly attenuated at almost all locations out of the high bay. Quasi-static pressures in this gastight model quickly equilibrated throughout the model (within 15-35 ms). The test data replicated very well, with all features of the complex time histories of pressure being essentially repeated during repeat tests, and small scatter in quasi-static pressure measurements.

During the Phase I testing, it quickly became apparent that quasi-static pressures for PBX 9404 explosive were considerably lower than predicted from methods in Ref. 2 which are based on TNT data and comparative heats of detonation of the two explosives. A summary of these measurements from the Phase I tests appear in Table 3.

In the Phase II testing, much more data were accumulated on quasi-static pressures, because explosive charge weight, test chamber volume and type of explosive were all varied. The average values for P_{QS} for all tests are plotted in Fig. 10 versus the "loading density" W/V. The line for TNT is reproduced from Ref. 2. Note that all data for PBX 9404 lie below the prediction line, while data for cylindrical and cased cylindrical charges lie above the line.

Table 1. Phase I Test Matrix

Test No.	Purpose	Charge	Blast Door Position	Charge Location
1 2 3	Instrumentation Testing	PBX 9404	Closed	Location A
0	Leakage Check	TNT	Closed	Location B
4 5 6	Equivalent Charge Location	PBX 9404	Closed	Location B
7 8 9	Load Verification	PBX 9404	Opened	Location B
10 11 12	Donor Bay Doors	PBX 9404	Closed	Location C

Table 2. Phase II Test Matrix

Test No.	Purpose	Charge	High Bay Door Position	Charge Location
14	Donor Bay Load	PBX-9404	Open	Location C
15-17	TNT Equivalence	TNT	Open	Location A
13, 18-22	TNT Equivalence	PBX-9404	Open	Location A
23-25	TNT Equivalence	PBX-9404	Open	Location A
27-29	Multiple Charges	PBX-9404	Open	Location D
30-31	Charge Geometry	PBX-9404	Open	Location A
32-39	TNT Equivalence	PBX-9502	Open	Location A
40-41	TNT Equivalence	PBX-9502	Closed	Location A
42-43	TNT Equivalence	PBX-9404	Closed	Location A
44-45	TNT Equivalence	Pentolite	Closed	Location A
46-47	TNT Equivalence	Pentolite	Open	Location A
48-50	Charge Confinement	PBX-9404	Open	Location A

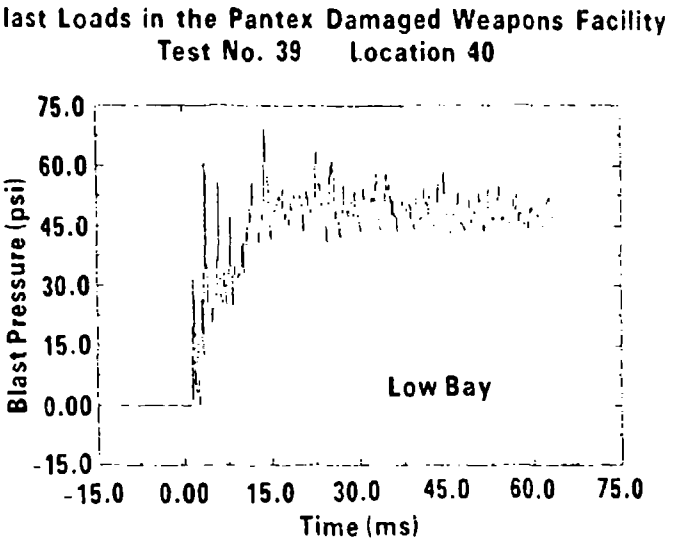

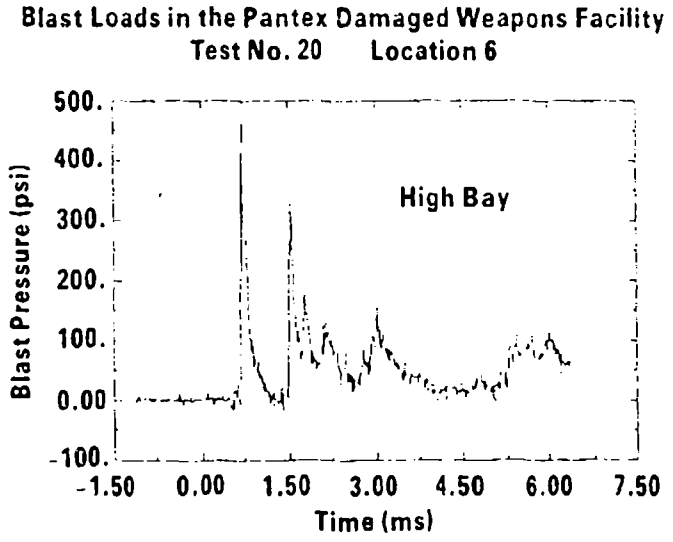

Figure 8. Blast Pressure Records

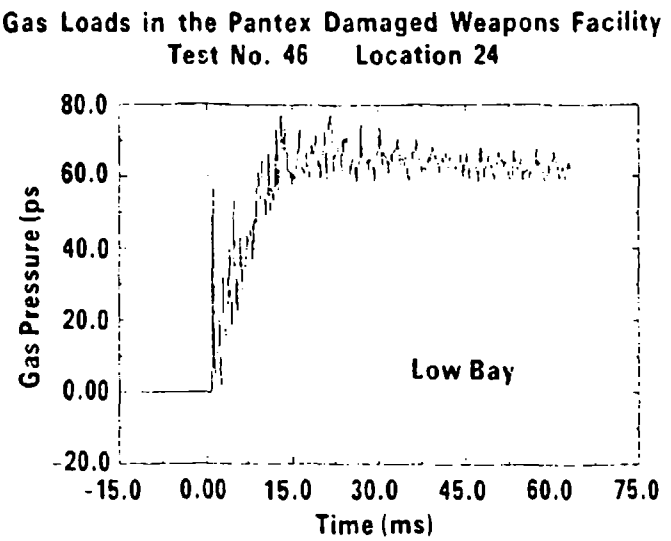

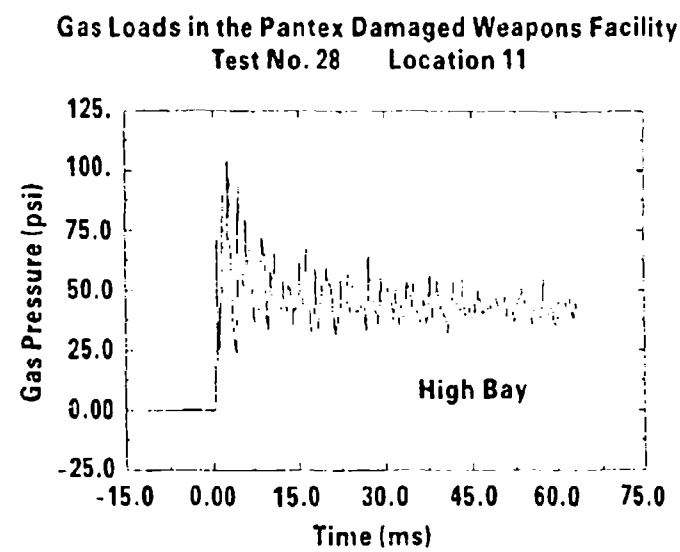

Figure 9. Gas Pressure Records

Table 3. Summary of Quasi-Static Pressure Measurements from Phase I Tests

Test No.	Blast Door Position	PQS (PSI) Estimated From Gas Gages PQS	S.D.	Blast Gages PQS	S.D.
1	Closed	43.3	1.1	41.2	6.3
2	Closed	49.1	2.0	51.7	6.0
3	Closed	45.9	0.7	48.6	8.1
4	Closed	46.9	4.2	44.4	4.6
5	Closed	41.0	0.9	46.2	6.4
6	Closed	43.7	2.7	46.0	7.1
10	Closed	51.5	5.5	50.6	6.1
11	Closed	47.3	1.5	44.7	5.1
12	Closed	49.7	3.5	–	–
		46.5 ± 3.4		46.7 ± 3.5	
7	Open	40.5	2.5	38.0	7.8
8	Open	40.1	1.6	39.5	4.3
9	Open	40.2	1.6	39.0	6.2
		40.3 ± 0.2		38.8 ± 0.8	
0	Closed (TNT)	77.0	6.3	85.4	10.5

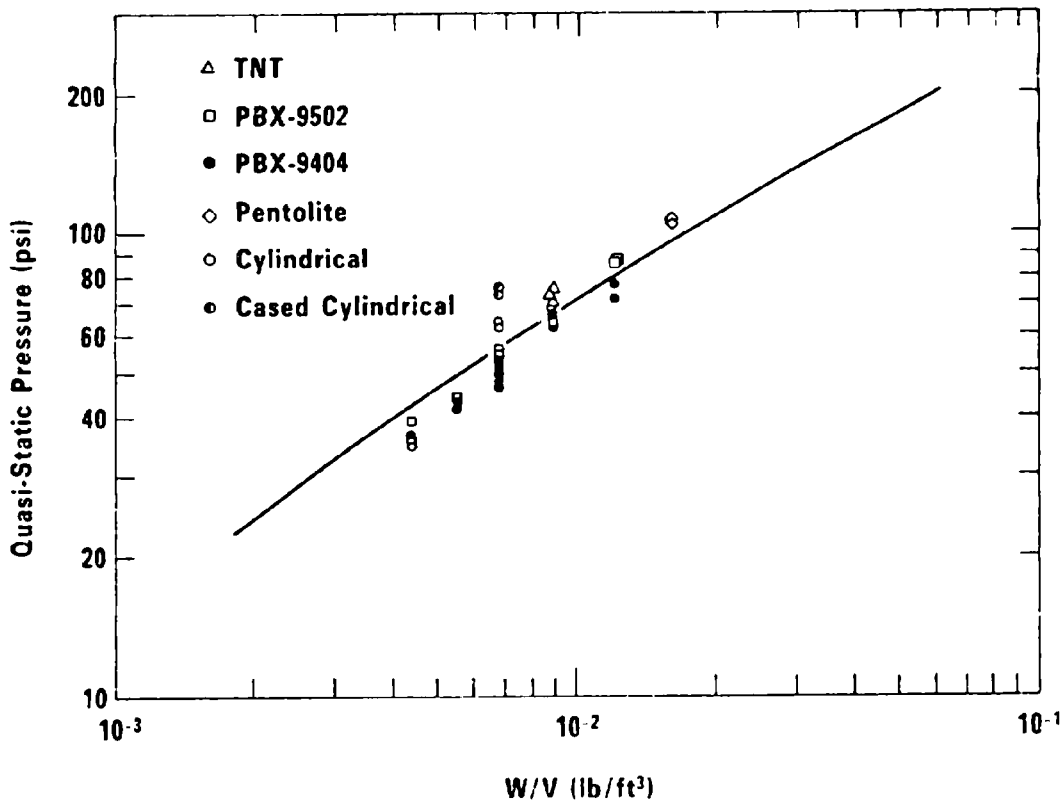

Figure 10. Summary of Quasi-Static Pressure Data

We realized that the quasi-static pressures in this range of loading density must depend on the heat of combustion of the explosive, as much as the heat of detonation, because there is enough oxygen in the air in the chamber to allow considerable afterburning and consequent heat addition to raise the pressure. Measurements of heats of combustion during Phase II allowed us to adjust the effective charge weights for the explosives, in a manner described in Ref. 5. The high quasi-static pressures for the cylindrical charges were at first puzzling, until we realized that both types of cylindrical charges had combustible plastic discs in intimate contact, and that the aluminum casing for the cased charges could also be partially combustible. Accounting for the effect of these energies on the quasi-static pressure allowed us to adjust the correlation with W/V, as shown in Fig. 11.

Unlike the quasi-static pressure data, there were no particular surprises in the shock pressure data. We did note, however, that the effects of changing charge geometry from spherical to cylindrical with L/D ratio of 1:1 were minimal. Also, the change from single spherical charges to pairs of spherical charges with the same total weight produced only minimal changes in shock pressure signals, for the particular charge location and gage measuring stations chosen in this program.

CONCLUSIONS

We can summarize by giving the major conclusions of the Phase I and Phase II testing as follows:

- Replication of tests yielded consistent results
- Shock loading is strongly attenuated by propagation through the highbay door into the lowbay
- The quasi-static pressure is independent of charge location
- The quasi-static pressure is dependent on the explosive type, explosive weight and the enclosed volume
- Cylindrical charges with L/D ratios of 1:1 produce shock loading similar to equal weight spherical charges
- For the configuration tested, multiple charges yield the same results as an equivalent single charge
- Material near the charge can substantially increase the quasi-static pressure.

The reduced data for shock loading on the walls of the high bay area are voluminous and could be used as a data base for verifying analytical or empirical shock loading prediction methods in design manuals. That task was not, however, part of the scope for this work.

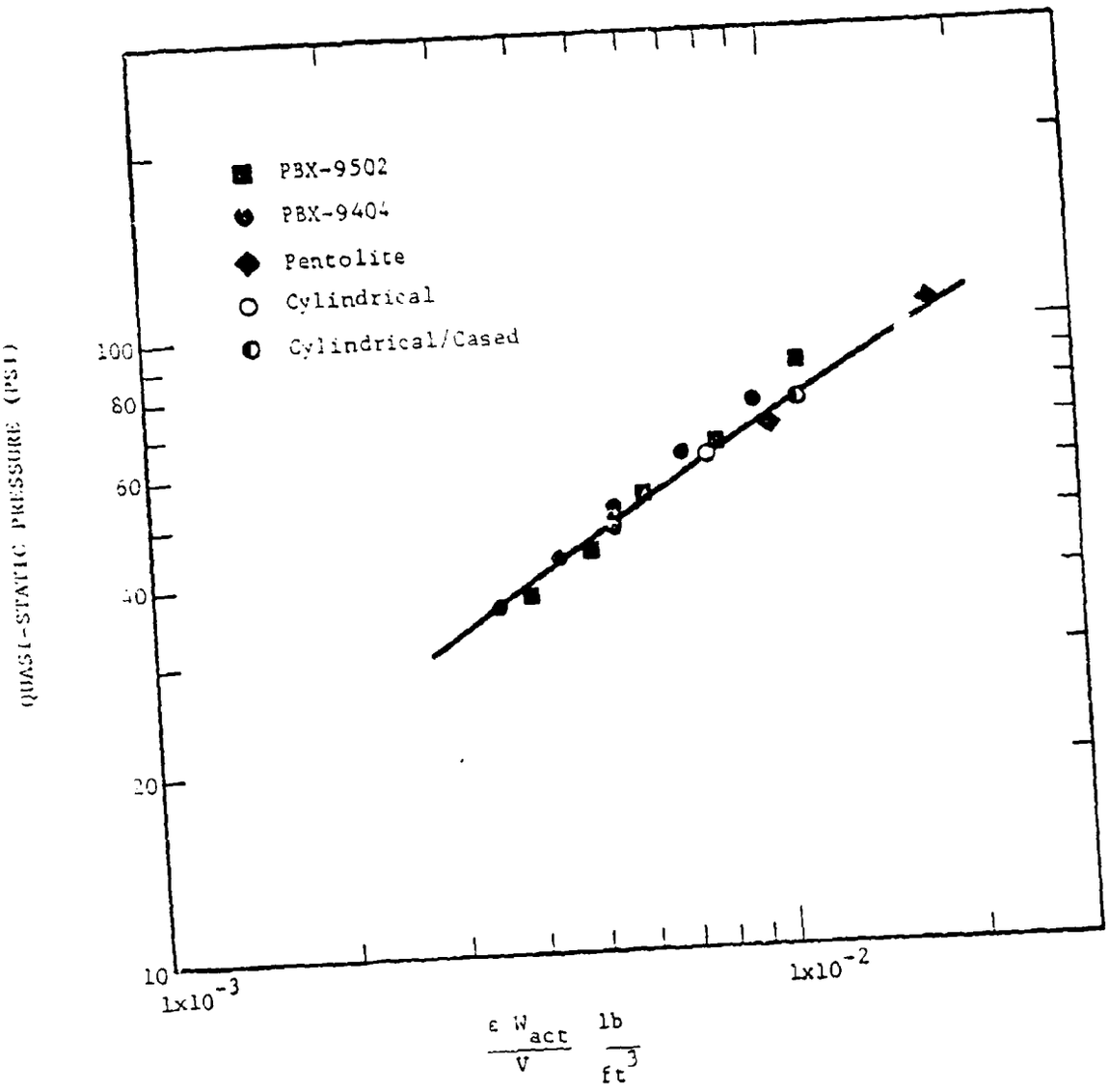

Figure 11. Quasi-Static Pressure versus Effective Charge to Volume Ratio

REFERENCES

1. Structures to Resist the Effects of Accidental Explosions (1969), Dept. of the Army Technical Manual TM5-1300, Department of the Navy Publication NAVFAC P-397, Department of the Air Force Manual AFM 88-22, Department of the Army, the Navy, and the Air Force, June 1969.

2. Baker, W. E., Westine, P. S., Kulesz, J. J., Wilbeck, J. S., and Cox, P. A., (1980) A Manual for the Prediction of Blast and Fragment Loadings on Structures, DOE/TIC-11268, U.S. Dept. of Energy, Albuquerque Operations Office, Amarillo Area Office, Amarillo, TX, Nov. 1980.

3. Hokanson, J.C., Esparza, E.D., Baker, W.E., and Sandoval, N.R., "Determination of Blast Loads in the Damaged Weapons Facility, Vol. 1, Final Report for Phase I," prepared for Mason and Hanger-Silas Mason Co., Inc., January 1982.

4. Hokanson, J.C., Esparza. E.D., Baker, W.E., and Sandoval, N.R., " Determination of Blast Loads in the Damaged Weapons Facility, Vol. 2, Final Report for Phase I," prepared for Mason and Hanger-Silas Mason Co., Inc., January 1982.

5. Hokanson, J.C., Esparza, E.D., Sandoval, N.R., Baker, W.E., and Anderson, C.E., "Determination of Blast Loads in the Damaged Weapons Facility, Vol. 1, Final Report for Phase II, " prepared for Mason and Hanger-Silas Mason Co., Inc., May 1982.

6. Hokanson, J.C., Esparza. E.D., Sandoval, N.R., Baker, W.E., and Anderson, C.E., "Determination of Blast Loads in the Damaged Weapons Facility, Vol. 2, Final Report for Phase II," prepared for Mason and Hanger-Silas Mason Co., Inc., May 1982.

7. Hokanson, J.C., Esparza, E.D., Sandoval, N.R., Baker, W.E., and Anderson, C.E., "Determination of Blast Loads in the Damaged Weapons Facility, Vol. 3, Final Report for Phase II," prepared for Mason and Hanger-Silas Mason Co., Inc., May 1982.

8. Baker, W.E., Westine, P.S., and Dodge, F.T., (1973) Similarity Methods in Engineering Dynamics: Theory and Practice of Scale Modeling, Spartan Books, Rochelle Park, NJ.

9. Suppressive Shields Structural Design and Analysis Handbook, (1977) HNDM-1110-1-2, U.S. Army Corps of Engineers, Huntsville, Division, November 1977.

10. Keenan, W.A., and Tancreto, J.E., (1974) Tech. Rept. 51-027, "Blast Environment from Fully and Partially Vented Explosions in Cubicles," Civil Engineering Laboratory, Naval Construction Battalion Center, Port Hueneme, California, February 1974.

11. Baker, W.E., Cox, P.A., Westine, P.S., Kulesz, J.J., and Strehlow, R.A., (1978) "A Short Course on Explosion Hazards Evaluation," Southwest Research Institute, San Antonio, Texas.

12. West, G.T., "Initiation of PBX 9404, Pentolite and TNT Spheres," Mason and Hanger Technical Report No. MH-SMP-82-01, December 1981.